

North Atlantic Modeling of Low-Frequency Variability in Mode Water Formation

AFONSO M. PAIVA

PEO, COPPE, Universidade Federal do Rio de Janeiro, Rio de Janeiro, Brazil

ERIC P. CHASSIGNET

Rosenstiel School of Marine and Atmospheric Science, University of Miami, Miami, Florida

(Manuscript received 9 January 2001, in final form 7 March 2002)

ABSTRACT

The generation of interannual and near-decadal variability in the formation of mode waters in the western North Atlantic is investigated in the realistic framework of an isopycnic coordinate ocean model forced with atmospheric data from 1946 to 1988. At Bermuda, the model reproduces quite well the observed potential vorticity and isopycnal depth anomalies associated with the subtropical mode water (STMW). Heat storage and preconditioning of the convective activity are found to be the important factors for the generation of STMW variability, with persistence of cold (warm) conditions, associated with anomalous heat loss (gain) over the western subtropics, being more significant for the generation of the simulated variability than are strong anomalous events in isolated years.

In the Labrador Sea, the model captures the phase and order of magnitude of the observed near-decadal variability in the convective activity, if not its maximum amplitude. The simulated potential vorticity anomalies are, as observed, out-of-phase with those in the western subtropics and correlate well with the North Atlantic Oscillation (NAO) at near-decadal timescales, with the oceanic response lagging the NAO by ~ 2 – 3 years. These results support the idea that the variability in water mass formation in the western North Atlantic can be attributed, to a large extent, to changes in the pattern of the large-scale atmospheric circulation, which generate sensible and latent heat flux variability by modifying the strength and position of the westerly winds and the advection of heat and moisture over the ocean. To the authors' knowledge, this is the first time that the interannual and near-decadal subsurface variability associated with STMW and Labrador Sea Water, and its relationship to the NAO, has been simulated in an ocean general circulation model.

1. Introduction

Understanding the processes associated with the observed low-frequency variability in the climate system of the North Atlantic has been a major concern of the scientific community in recent decades (ACCP 1992; WCRP 1995). Several studies have been carried out in order to investigate the mechanisms responsible for the observed sea surface temperature (SST) variability (e.g., Bjerknes 1964; Deser and Blackmon 1993; Kushnir 1994; Delworth 1996). These studies were motivated in part by the important role played by SST in the coupling between ocean and atmosphere, and were made possible by the availability of observational datasets [such as the Comprehensive Ocean–Atmosphere Data Set (COADS)] representing the SST variability on interannual and longer timescales.

Recently, there has been increasing interest in inves-

tigating the long-term variability in subsurface layers of the ocean, since it is recognized that this variability may in turn affect the SST variability. It has been demonstrated, for example, that winter SST anomalies can be preserved in the seasonal thermocline below the summer mixed layer and may reappear at the surface in subsequent winters (Alexander and Deser 1995). Subducted anomalies, which are transported away from their formation region by the large-scale circulation, can also feed back upon the surface in remote regions, establishing teleconnections that may account in part for the long-term memory of the ocean (Latif and Barnett 1994). Zhang et al. (1998) tracked anomalous warm water from the subduction region of the midlatitude North Pacific to the Tropics, from the early to the late 1970s, and suggested that these anomalies may have influenced the El Niño events of the 1980s. Decadal variations in the formation rates and properties of Labrador Sea Water (LSW) have been traced to intermediate depths in the western North Atlantic midlatitudes with a time delay of approximately 6 years (Curry et al. 1998).

Observations of long-term subsurface variability in

Corresponding author address: Dr. Eric P. Chassignet, RSMAS MPO, University of Miami, 4600 Rickenbacker Causeway, Miami, FL, 33149-1098.
E-mail: echassignet@rsmas.miami.edu

the North Atlantic (e.g., Levitus 1989) are sparse (both in space and in time), and evidence of the associated forcing mechanisms is not yet conclusive. Only a few locations, which have been continuously monitored, provide long-term records of water mass properties. Based on analysis of data from the Panulirus station ($32^{\circ}10'N$, $64^{\circ}30'W$), located in the western subtropical gyre, variability on interannual to near-decadal time-scales in the formation rates and properties of Subtropical Mode Water (STMW), or 18° Water, has been shown to occur (Talley and Raymer 1982; Joyce and Robbins 1996). STMW is formed by subduction through the base of the winter mixed layer, in a region of strong surface heat loss. Expecting the observed variability to be caused by changes in surface forcing, and consequently in convective activity, Jenkins (1982) and Talley and Raymer (1982) were however unable to strongly correlate this variability to surface heat flux anomalies. Notwithstanding these results, Marsh and New (1996) and Hazeleger and Drijfhout (1998) were able to simulate the changes in potential vorticity (PV) observed to occur in the STMW core in the 1960s and 1970s by forcing a numerical model with idealized heat flux anomalies. Talley (1996), however, notes that the observed PV anomalies of STMW are well correlated with the anomalies in sea surface salinity (SSS), invoking nonlocal advective processes to explain the variations observed in the data. Long-term records from OWS Bravo ($56^{\circ}30'N$, $51^{\circ}00'W$), in the central Labrador Sea, demonstrate that the formation rates and properties of LSW also have nonstationary characteristics (Lazier 1981; Talley and McCartney 1982; Lazier 1988). The thickness and potential temperature of LSW have been shown to possess negatively correlated near-decadal variations (Curry et al. 1998). Low production of LSW corresponds to periods of weak surface heat loss in the Labrador Sea (McCartney and Talley 1982), and also to the occurrence of intense freshwater surface anomalies that enhance the vertical stratification and reduce convection (Lazier 1981).

It has been noted (Dickson et al. 1996; Houghton 1996; Joyce et al. 2000) that the decadal variability in convective activity in the North Atlantic western subtropical gyre and in the Labrador Sea have near opposite phases. Dickson et al. (1996) suggest that this asynchronicity is imposed by the spatial and temporal scales of the atmospheric forcing, which can be characterized by referring to the North Atlantic Oscillation (NAO). When the NAO index (the pressure difference between the Azores high and Iceland low atmospheric systems) is high, the heat loss is intense in the Labrador Sea due to strong westerlies and cold air advection, but is low in the western subtropical gyre due to the inflow of warm and moist air (Cayan 1992); when the NAO index is low, the westerlies shift southward, intensifying the storminess (Dickson and Namias 1976; Rogers 1990) and the outbreaks of cold and dry continental air over

the western subtropics, thus enhancing the heat loss in that region and reducing it in the Labrador Sea.

In the present study, the generation of interannual and near-decadal variability in the formation of mode waters in the western North Atlantic is investigated in the realistic framework of an ocean general circulation model (OGCM) forced with monthly atmospheric COADS fields from 1946 to 1988. The objectives of this work are (i) to evaluate which part of the observed and simulated variability can be attributed to changes in the upper-ocean buoyancy, in particular those changes related to surface heat flux variability, and (ii) to investigate to what extent the heat flux anomalies contribute to the observed phase differences between the convective activity in the western subtropical and subpolar basins. The model setup and the atmospheric forcing fields are described in section 2. Results from the numerical simulations are presented in section 3 for the simulated surface anomalies, in section 4 for the variability in the renewal of STMW in the western subtropics, and in section 5 for the intensity of convection in the Labrador Sea. The results are then summarized and discussed in section 6.

2. Model configuration and forcing

The ocean numerical model is the Miami Isopycnic Coordinate Ocean Model (Bleck et al. 1992; Bleck and Chassignet 1994), configured with realistic topography and stratification. The computational domain is the North and equatorial Atlantic Ocean basin from $28^{\circ}S$ to $65^{\circ}N$, including the Caribbean Sea and the Gulf of Mexico. The bottom topography is derived from a digital terrain dataset with $5'$ latitude–longitude resolution (ETOPO5) by averaging the topographic data located in each grid box. The horizontal grid is defined on a Mercator projection with resolution given by $1^{\circ} \times 1^{\circ} \cos(\phi)$, where ϕ is the latitude. The vertical density structure is represented by 15 isopycnic layers (σ_{θ} values of 24.70, 25.28, 25.27, 26.18, 26.52, 26.80, 27.03, 27.22, 27.38, 27.52, 27.64, 27.74, 27.82, 27.88, and 27.92), topped by a dynamically active Kraus–Turner surface mixed layer. The vertical discretization was chosen to provide maximum resolution in the upper part of the ocean. In such a model, the water mass formation can be unequivocally related to mass exchanges between the surface mixed layer and the subsurface layers.

Open ocean boundaries are treated as closed, but are outfitted with buffer zones 3° wide in which temperature T and salinity S are linearly relaxed toward their seasonally varying climatological values (Levitus 1982). The buffer zones restore the T and S fields to climatology in order to approximately recover the vertical shear of the currents through geostrophic adjustment. At the surface, the model is driven by both mechanical and diabatic forcing. The momentum flux is given by the longitudinal and latitudinal components of the wind stress and the mixed layer stirring rate by the oceanic

friction velocity. The thermodynamic forcing consists of the heat flux (radiative plus turbulent) implemented with the bulk formulations computed with prescribed atmospheric variables and model SST, and of the freshwater flux (evaporation minus precipitation, which is implemented as a virtual salt flux and is independent of the model solution) [see Paiva and Chassignet (2001) for details]. Freshwater river runoffs are implemented by adding observed values, based on Perry et al. (1996), to the precipitation field at the grid point nearest to the river mouth.

The model was initialized from the Levitus (1982) climatology and was spun up from rest for a total of 20 years with atmospheric data derived from the COADS monthly climatology (da Silva et al. 1994). A detailed discussion of the spinup can be found in Paiva and Chassignet (2001). After the spinup phase, the model was integrated for an additional 43 years by adding monthly atmospheric anomalies from the year 1946 to 1988 to the climatological forcing used in the 20-yr spinup. A smooth transition from the climatological forcing was obtained by linearly weighting the anomalous fields in the initial year, with weights varying from 0 to 1 from January to July.

In a first experiment (hereafter EXPI), monthly variability was added to the wind stress (τ'), to the friction velocity (u_*'), to the wind speed (W'), to the air temperature (T'_a), and to the specific humidity (q'_a). The prescription of atmospheric variables in the heat flux formulation implies a restoring of the model SST toward a prescribed equilibrium temperature (Paiva and Chassignet 2001) and does not allow for the atmosphere to respond to oceanic SST anomalies (Luksch and von Storch 1992; Seager et al. 1995, 2000). Observational and numerical evidence (Cayan 1992; Kushnir 1994; Delworth 1996; Halliwell 1998; Seager et al. 2000), however, indicate that in the North Atlantic, on the time-scales of interest in this study (interannual to near-decadal), the variability in the buoyancy of the upper ocean associated with SST anomalies is primarily an oceanic response to anomalous atmospheric forcing, with surface heat flux anomalies dominating over horizontal advection and vertical mixing variability. Our strategy is analogous to that used by Battisti et al. (1995) and Häkkinen (1999), with the T'_a and q'_a fields including the effects of horizontal atmospheric advection, which is important in the present study for the representation of continental air outbreaks over the ocean.

Atmospheric W' , T'_a , and q'_a lead to variations in the sensible (Q'_s) and latent (Q'_l) heat fluxes. The variance of Q'_s and Q'_l has been shown by Cayan (1992) to dominate that of the radiative fluxes during wintertime in the extratropics when the formation of mode water occurs through subduction and/or convection (Marshall et al. 1993; Marshall and Schott 1999). The largest Q'_l occurs from the Tropics to midlatitudes and the largest Q'_s from mid to high latitudes, while at mid latitudes Q'_l and Q'_s are strongly correlated and tend to be rein-

forcing (since cooler air is usually dryer). The surface freshwater flux is prescribed from the COADS monthly climatology (i.e., no anomalies). The modeled sea surface salinity is therefore not constrained to remain close to climatological values (Paiva and Chassignet 2001) and the generated SSS anomalies (hereafter SSS') are free to propagate.

In order to isolate those changes in subsurface variability that are due to local atmospherically forced convective anomalies from those possibly due to displacement of isopycnal surfaces associated with variability in the Ekman pumping and/or in the intensity of the wind driven gyres [as observed by Miller et al. (1998) in the North Pacific], two additional experiments were performed. In EXP II, the surface forcing is that of EXPI with the exception of the wind stress, which in EXP II has only the climatological component. In contrast, anomalies only of wind stress are considered in EXP III, while the remainder of the forcing is based on the seasonal climatologies.

Studies concerning SST variability generally focus on wintertime atmospheric and oceanic conditions since the low stratification makes SST a good indicator of the upper-ocean heat content (Cayan 1992). The present study also focuses on the wintertime surface fields since these determine the properties of the newly formed water masses. Subsurface variability is, however, characterized by summer conditions (when the mixed layer is shallower), which most likely indicate the water mass properties acquired by subduction and/or convection in the previous winter. Results from the model simulations were archived monthly and were analyzed for the period from 1947 to 1988. In order to generate anomalies of the simulated fields, monthly mean values (for the 42-yr period with anomalous forcing) were subtracted from the model data at each grid point, and a linear trend was further removed from the resulting time series.

3. Surface variability

In this section, the simulated anomalies of sea surface temperature (hereafter referred to as SST') and of the surface heat flux are presented and discussed. Since the focus of this study is on the generation of subsurface variability, one needs to first evaluate the model skills in reproducing the observed surface anomalies, which induce variability in the surface layer buoyancy and in water mass formation.

Previous studies (Bjerknes 1964; Kushnir 1994) have pointed out that the observed SST' patterns in the North Atlantic are coherent in the zonal direction. In order to provide a visual impression of the amplitude and time-scales of the SST variability, a comparison of the wintertime (January–March average) SST' from the model and the observations, averaged in 10° wide latitude bands, is shown in Fig. 1. The SST' order of magnitude is 1°C, and variations with biannual and near-decadal timescales are clearly discernible. Longer timescales are

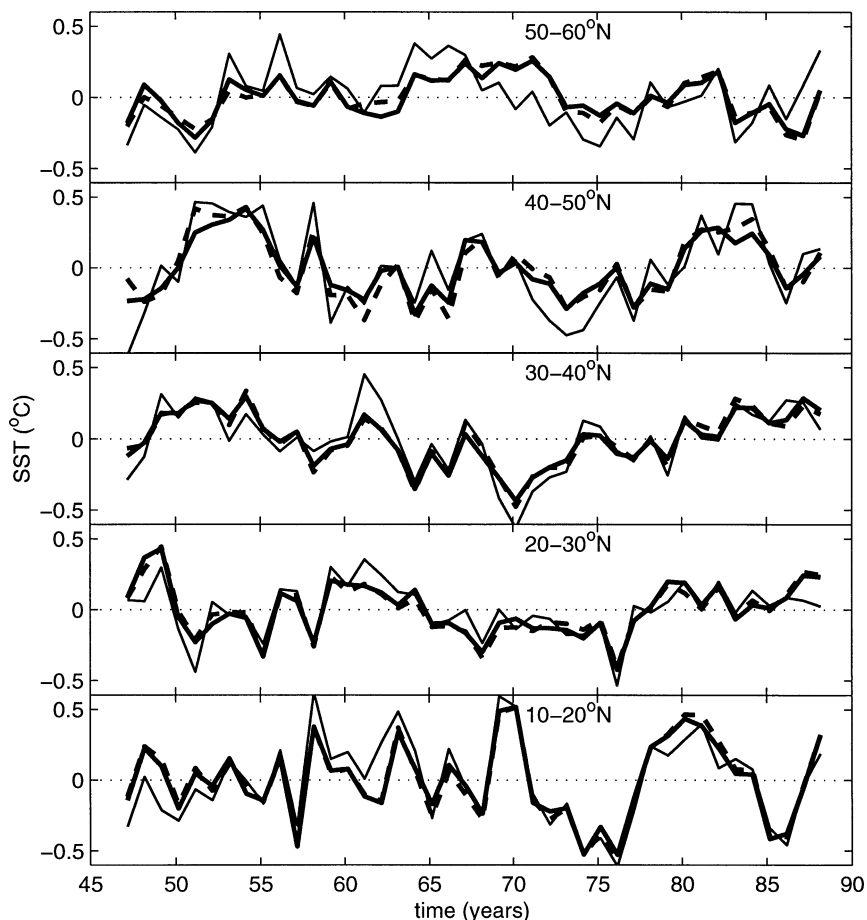


FIG. 1. Zonally averaged (in 10° lat bands) wintertime SST anomalies: observations (thin solid lines), EXPI (thick solid lines), and EXPII (thick dashed lines).

also apparent in this figure, which shows the warm (1950s) and cold (1970s) periods in the extratropics that were documented by Kushnir (1994). As demonstrated in Fig. 1, EXPI captures reasonably well the time and amplitude scales of the variability seen in the observations. The poorest agreement is that in the 50°–60°N zonal band around 1970, when the model SST' has a weaker amplitude than that observed and the intense cooling in the model lags observed values by ~2–4 years. Analysis of individual time series (not shown) indicates that the mismatch occurs primarily in and near the Labrador Sea, which in reality (though not in the model) was the site of the “Great Salinity Anomaly” at that particular time (Dickson et al. 1988).

The skill of the model in simulating SST' is also attested to by high values of the correlation coefficient between observed and simulated SST anomalies (not shown). The distribution of the correlation coefficient over the model domain is very similar to that obtained by Battisti et al. (1995) and Häkkinen (1999), with values greater than 0.4 over most of the domain (coefficients greater than or equal to 0.39 are statistically significant at the 99% level). The model performs partic-

ularly well in mid latitudes, to the south and southeast of the Gulf Stream and North Atlantic currents (where correlation coefficients exceed 0.6–0.8), which are the regions in which mode waters are ventilated in the subtropical gyre (McCartney 1982). Lower correlations occur at higher latitudes, in the vicinity of the lateral buffer zones, in which surface properties are relaxed toward climatological values derived from Levitus (1982), thus inhibiting the development of the SST anomalies. In the Labrador Sea and east of Newfoundland, an additional factor leading to the lower correlation is possibly the effect on the observed SST anomalies of ice melting (Deser and Blackmon 1993), which is not incorporated in the present study. The correlation between observed and simulated SST' is improved everywhere in the North Atlantic during summer, a result also obtained by Battisti et al. (1995) and Häkkinen (1999).

In order to better describe the basin-scale modes of SST variability, an EOF analysis was carried out for the observed and simulated anomalous fields. The first two EOFs of simulated SST' account for 25% and 15% of the total variability, respectively, and agree well with the first two modes computed from observations. The spatial

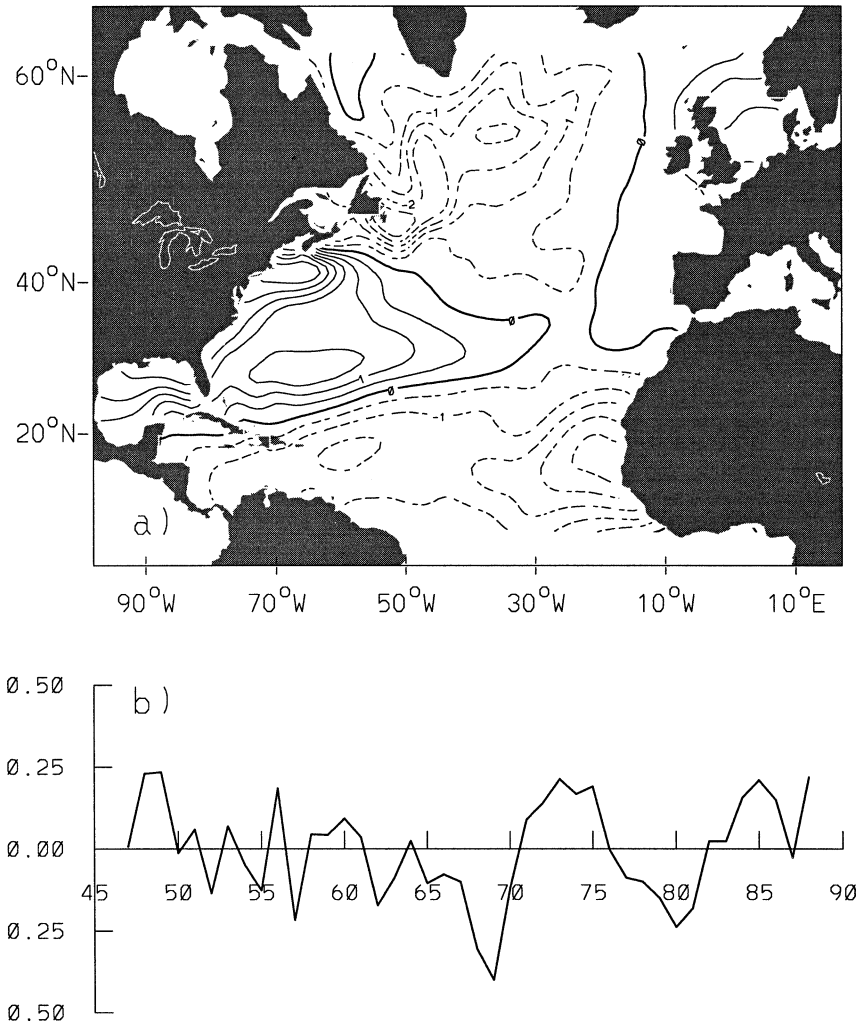


FIG. 2. (a) EOF 1 [solid (dashed) lines are positive (negative) contours; the contour interval is 0.5°C] and (b) time series of EOF 1, of model (EXPI) wintertime SST anomalies.

distribution and time series of the first EOF derived from the model results (hereafter EOF1 SST) are shown in Fig. 2. The dipole pattern at mid and high latitudes, with greater variability in the western basin, resembles that of the second EOF in the analysis of Deser and Blackmon (1993). Note that these authors considered data from the beginning of the century so that their first EOF is dominated by a centennial timescale with single polarity in the entire basin. The spatial pattern of EOF1 SST is also representative of the composite analysis (the difference between warm and cold years) of Kushnir (1994) and Battisti et al. (1995). The time series of EOF1 SST shown in Fig. 2 also displays biannual and near-decadal oscillations, which are observed in the zonally averaged SST' presented in Fig. 1.

Another indicator of model performance is the surface heat flux. The first EOF of the surface heat flux variability derived from the model results (hereafter EOF1 HFLX), which accounts for 38% of the total variability

in the data is shown in Fig. 3, and agrees well with an EOF analysis performed with the COADS observations (not shown). Both the spatial pattern and timescales of EOF1 HFLX and EOF1 SST are highly similar, with positive heat flux anomalies into the ocean corresponding to SST warming and negative heat flux to SST cooling. EOF1 HFLX is also in very good agreement with the first EOF of latent plus sensible heat flux variability presented by Alexander and Scott (1997), simulated in an atmospheric model forced with climatological SST, thus suggesting that EOF1 HFLX is representative of an internal mode of variability in the atmosphere. This mode has been associated with the existence of variations in the atmospheric circulation correlated to the NAO (Zorita et al. 1992; Kushnir 1994). A dipole pattern in the buoyancy of the wintertime mixed layer of the ocean (associated with EOF1 SST) is consistent with a scenario in which atmospheric forcing (characterized by EOF1 HFLX) leads to the observed out-of-phase

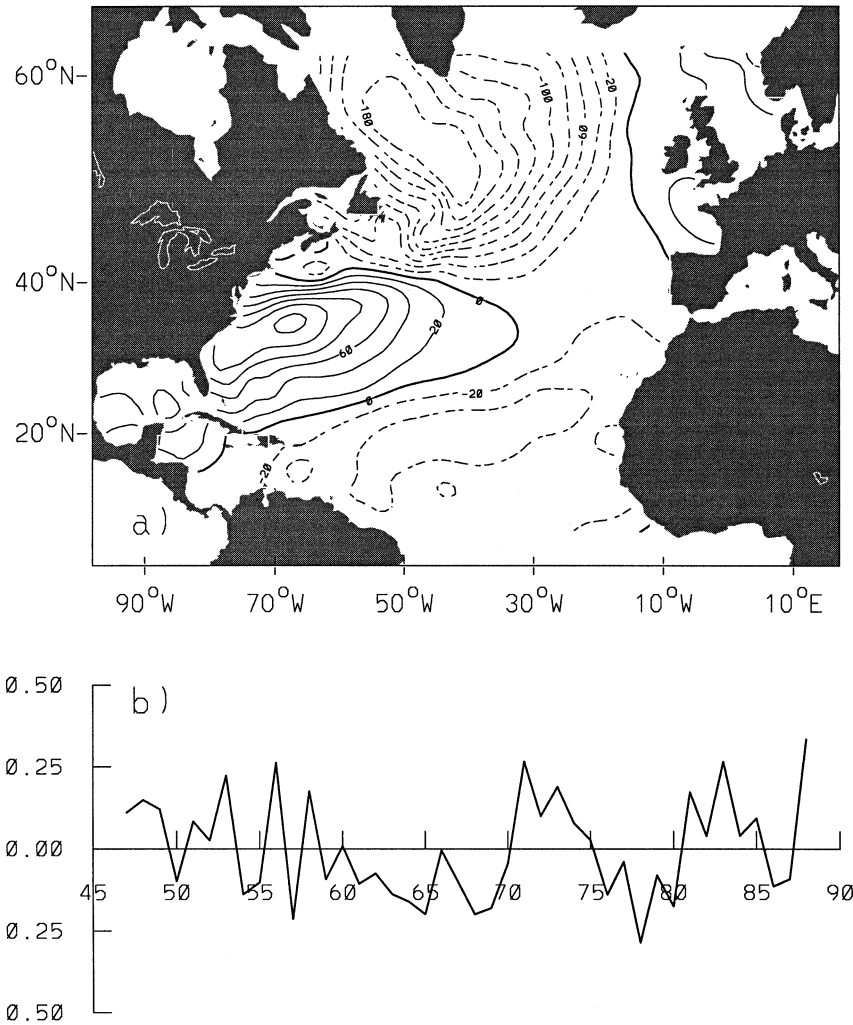


FIG. 3. (a) EOF 1 [solid (dashed) lines are positive (negative) contours; the contour interval is 20 W m^{-2}] and (b) time series of EOF 1, of model (EXPI) wintertime surface downward heat flux anomalies.

variability in the water mass formation in the Labrador Sea (LSW) and in the western Atlantic (STMW).

The SST' simulated in EXP II are comparable to those in EXP I, as shown in Fig. 1. Both the correlation coefficients between the simulated and observed anomalies and the EOF modes of SST' and heat flux anomalies in EXP II (not shown) are also highly similar to those of EXP I. These results are consistent with those of Battisti et al. (1995) and Delworth (1996), which show that the magnitude of the SST' can be quantitatively accounted for by the heat flux anomalies, while the oceanic advection plays only a secondary role. In EXP III (which is forced with anomalies of the wind stress but not of the heat flux), the simulated SST' are very weak (not shown) and concentrated primarily along the Gulf Stream, and the correlation coefficients between the simulated and observed SST' (not shown) are below (or close to) the significance levels over the entire domain. This result is not unexpected since, in that experiment,

the heat flux formulation implicitly restores the model SST to climatology, thereby inhibiting the development of SST anomalies (Seager et al. 2000; Paiva and Chassignet 2001).

EXP III is useful, however, to shed some light on the processes associated with the sea surface salinity anomalies (SSS'), the variability of which is directly related to variations in the advective fields since the sea surface salinity is not constrained by observations (Paiva and Chassignet 2001) and no $E - P$ anomalies are present in the forcing. Near-decadal variations in the Gulf Stream transport, with magnitude $\sim 5 \text{ Sv}$ ($\text{Sv} \equiv 10^6 \text{ m}^3 \text{ s}^{-1}$), are observed in EXP III as a consequence of the variability in wind stress curl over the subtropical gyre. While there are no continuous direct measurements of Gulf Stream transport variability to which to compare the model results, hydrographic data indicate that the Gulf Stream was weaker in the early 1970s than in the late 1950s by $\sim 6 \text{ Sv}$ (Sato and Rosby 1995) and that

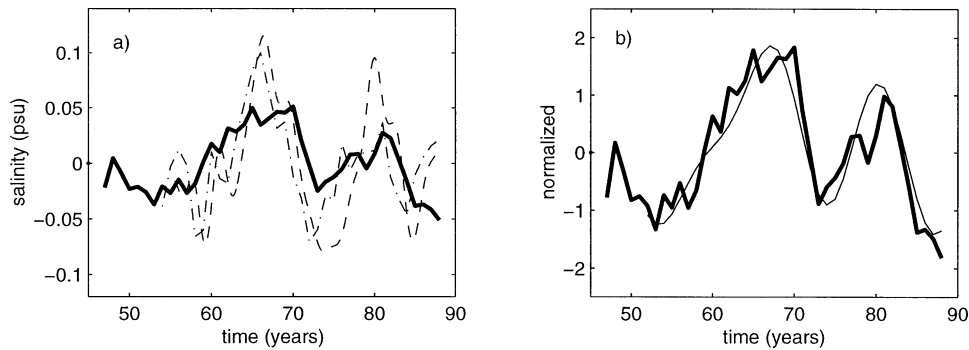


FIG. 4. (a) Salinity anomaly at Bermuda in EXP111 (thick solid line) and from observations: dashed-dotted line from Joyce and Robbins (1996) for the 0–200-m depth interval, and dashed line from L. D. Talley (1999, personal communication) for $\sigma_{\theta} = 26.2$. (b) Salinity anomaly at Bermuda (thick solid line) and Gulf Stream transport anomaly (thin solid line) lagged by 3 yr, in EXP111. Both curves in (b) are normalized by their respective standard deviations. The transport anomaly has been smoothed with a low-pass filter with cutoff frequency of 8 yr.

it strengthened around 1975 (Worthington 1977), in agreement with the simulated variations. SSS anomalies simulated near Bermuda in EXP111 have phase similar to that of the observed anomalies (Fig. 4a) for the near-decadal signal. These anomalies correlate well with the simulated transport variability for a 3-yr time lag (Fig. 4b), in agreement with the Talley (1996) hypothesis of an advective source for the salinity variations at Bermuda. It is unclear, however, if the weaker magnitude of the simulated SSS', when contrasted to observations, reflects the absence of surface freshwater flux anomalies in the model or deficiencies in the model advective field.

4. Subtropical mode water variability

Subtropical Mode Water (STMW) is a major constituent of the upper thermocline in the western subtropical gyre (Worthington 1959). Its formation is associated with subduction through the base of the shoaling mixed layer at the offshore flank of the Gulf Stream, and its vertical homogeneity is acquired through deep convection driven by intense wintertime buoyancy loss (McCartney 1982). In this section, the model results representing the simulated STMW variability under anomalous atmospheric forcing are compared to observations, and the importance of the surface heat flux in generating the observed variability is assessed.

In the present simulations, of the model layers that exist in the North Atlantic subtropical gyre, only layers 5 ($\sigma_{\theta} = 26.18$), 6 ($\sigma_{\theta} = 26.52$), and 7 ($\sigma_{\theta} = 26.80$) are ventilated directly in the western portion of the gyre. The time evolution of the vertical layer structure at the model grid point closest to the location of the Panulirus station is shown for EXP111 in Fig. 5a. A bias toward higher than observed SSS in the subtropics (Paiva and Chassignet 2001), simulated during the spinup phase, contributes to an upward migration of the isopycnals and to the simulation of denser than observed STMW (which is represented in the model by layer 7).

The low-frequency variability in the STMW at Panulirus is manifested in the model by variations in the relative amount of mass (thickness) of layers 6 and 7 and by the corresponding variations in the depth of the interface between these two layers, as seen in Fig. 5a. The Talley and Raymer (1982) time series of observed isopycnal depths at Panulirus (their Fig. 4) is reproduced here in Fig. 5b, with the data extended through the 1980s (Talley 1999, personal communication) and overlaid by the time series of the model summer interface depth. As shown in this figure, the model reproduces quite well the near-decadal oscillations present in the data. These oscillations are characterized by the accentuated shoaling of the isopycnals observed to occur from approximately 1964 to 1971, and to a lesser extent in the late 1970s, separated by a period of deeper isopycnals similar to that seen in the initial part of the observed and simulated records.

A useful mode water tracer (McCartney 1982) is its potential vorticity (PV), which for negligible relative vorticity can be defined as

$$\frac{f}{\rho_0} \frac{\partial \rho}{\partial z}, \quad (1)$$

where f is the Coriolis parameter, ρ_0 a reference density, and the partial derivative denotes the vertical density gradient. By virtue of their vertical homogeneity (and low density gradient), mode waters are characterized by a PV minimum in the water column, with negative (positive) PV anomalies indicating greater (smaller) than average formation of a particular mode water. A discretized version of Eq. (1) (New et al. 1995) was computed for layer 7, representing summer conditions, and the time evolution of the model STMW PV anomaly (hereafter referred to as PV') is shown in Fig. 5c. The low-frequency variability agrees well with that observed by Talley and Raymer (1982) in their representation of the STMW PV anomaly in density space for the 1954–

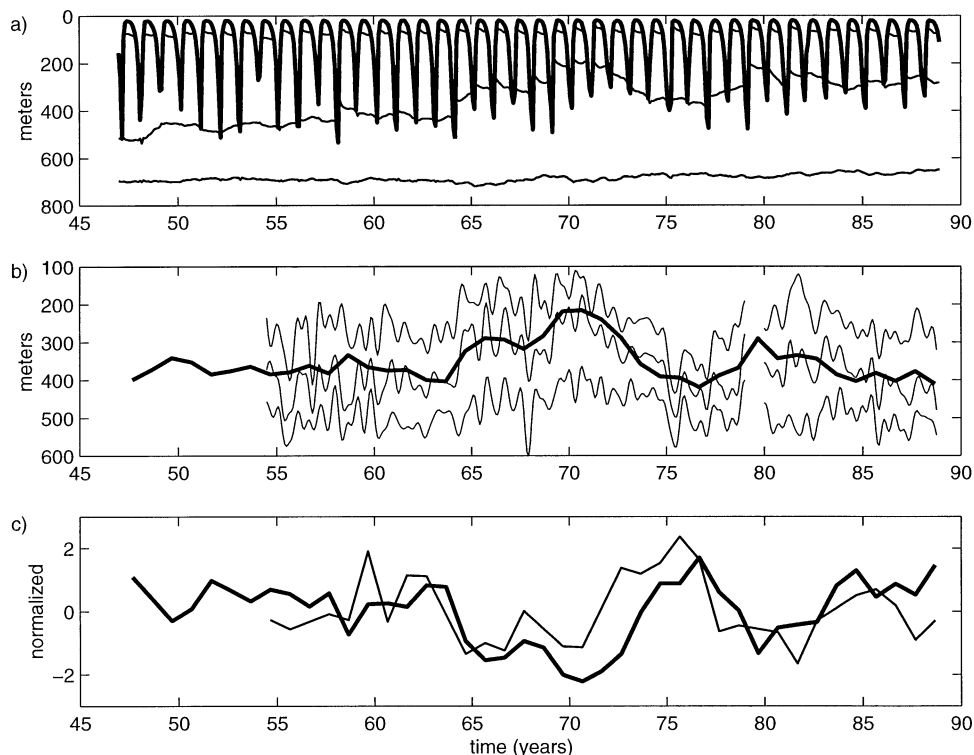


FIG. 5. Time evolution at Bermuda for (a) model (EXPI) layer structure (thick line is the base of the mixed layer, and thin lines are the base of layers 5, 6, and 7, from top to bottom); (b) depth of interface between model (EXPI) layers 6 and 7 in Sep, detrended and added to its mean value (thick line), and observed depth of 26.4, 26.5, and 26.6 (from top to bottom) σ_θ surfaces (thin lines), from L. D. Talley (1999, personal communication); and (c) potential vorticity anomaly of model (EXPI) layer 7 (thick line), and from observations (thin line) within the depth range 200–400 db (Joyce and Robbins 1996), normalized by their respective standard deviations.

78 period (their Fig. 3). Both in the observations and in the model, there is an indication of (i) a period of relatively uniform conditions prior to the early 1960s, which in the model exists from the late 1940s, prior to the time of the observations; (ii) an intensification of the ventilation around 1964, with negative PV' and increased production of a denser mode water persisting until approximately 1971; (iii) a comparatively abrupt and intense reduction of the ventilation, with an overall PV maximum for the entire period of observations near 1975; and (iv) a recovery of the ventilation and PV conditions characteristic of the initial part of the record to the 1980s.

For comparison, Fig. 5c also includes the PV anomalies in the dbar pressure range 200–400, based on observations, redrawn from Joyce and Robbins (1996). While the curves in Fig. 5c compare well, there is an indication that the model PV' lags that of the observations by ~1–2 years. Whether this lag is a real feature, or an artifact arising from the different ways in which the two curves were computed, is unclear. If real, it could indicate a delayed response of the model to the forcing, or simply the fact that the Panulirus location in the model is not identical to that in reality, with

respect to the simulated and observed circulation of the western subtropical gyre.

From Fig. 5a, it is apparent that there is little correlation between the simulated PV (or the interface depth) anomaly at Bermuda and the local convective activity, as expressed by the depth of the simulated wintertime (March) mixed layer (the correlation coefficient is 0.2). Marsh and New (1996) found similar results analyzing data from the Panulirus station. When the PV anomalies at Bermuda are correlated to the depth of the March mixed layer at different model grid points in the western Atlantic, the correlation coefficients are observed to increase in the northeast direction, reaching a maximum of 0.68 at 36°N, 60°W. This is consistent with STMW not being formed at Bermuda, but rather being advected through the location of the Panulirus station by the recirculation of Gulf Stream water in the Sargasso Sea (Fieux and Stommel 1975; McCartney 1982). As will be shown in the remainder of this section, the low-frequency signal of the STMW PV' observed in the model results is, in fact, generated northeastward of Bermuda and is advected by the mean flow through the location of the Panulirus station.

The correlation coefficients between PV' at Bermuda

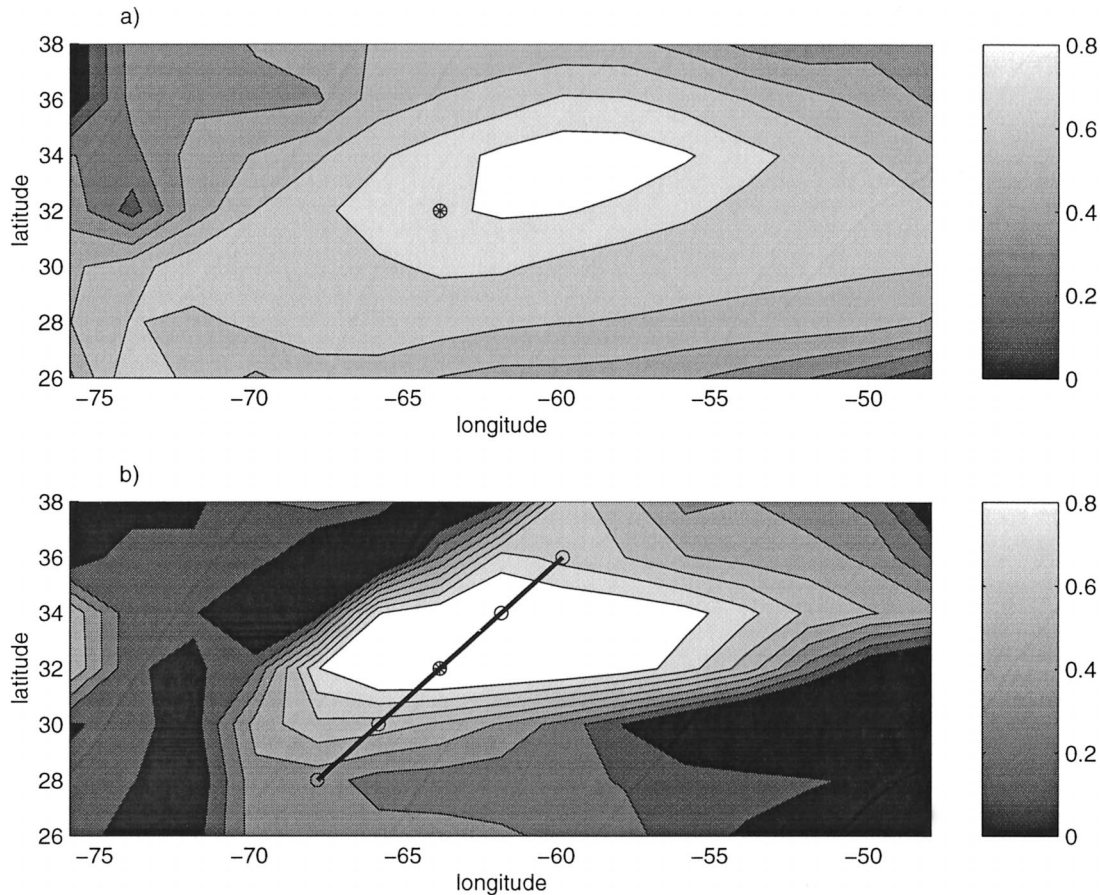


FIG. 6. (a) Correlation coefficient between the PV' of STMW (layer 7) at Bermuda in EXPI and the wintertime SST' in the western subtropics (contour interval 0.1). (b) As in (a) but for PV' at Bermuda and layer 7 PV' in the western subtropics. The filled circle is the position of Bermuda. The open circles along the segment line are the positions used in the PV' computations shown in Fig. 8.

and SST' over the western subtropical gyre are shown in Fig. 6a, with the maximum correlation of 0.87 observed to occur northeast of Bermuda. Wintertime SSS anomalies are weak in EXPI, and SST' is a good indicator of the density (and buoyancy) variability of the mixed layer. The fact that PV' at Bermuda correlates better with SST' than with mixed layer depths indicates that the controlling factor in the STMW variability is not so much the depth of wintertime convection as the density of the mixed layer, which determines the partitioning of the subducted water among the model layers that are ventilated in the western subtropical gyre. The correlation coefficients in Fig. 6a are above the 99% significance level over a large area in the western Atlantic, as expected, since SST anomalies in the model and in observations have spatial scales on the order of ~ 1000 km in the subtropics.

In order to represent the spatial scales of the simulated PV anomalies, we have correlated the time series of PV' at Bermuda (Fig. 5c) with PV' computed in a similar way at different model grid points over the western Atlantic (Fig. 6b). The variability simulated at Bermuda

is coherent over a large area in the Sargasso Sea limited to the northwest by the Gulf Stream front (the position of which corresponds roughly to the 0.6 contour in Fig. 6a, and to the 0.2 contour in Fig. 6b) and extending to $\sim 50^\circ W$, $\sim 28^\circ N$. This result is corroborated by a principal component analysis carried out for the anomalies of the depth of the interface between layers 6 and 7 (Fig. 7), representing summer conditions. While the time series of the first EOF mode (Fig. 7b), which accounts for 38% of the total variance, captures the near-decadal oscillations observed and simulated at Panulirus (Fig. 5b), its spatial distribution (Fig. 7a) shows the maximum variability to be centered to the northeast of Bermuda (where wintertime convection is at a maximum), whence it spreads primarily to the south and southwest in the Sargasso Sea.

In order to follow the evolution and propagation of the STMW PV anomaly, Fig. 8 shows the PV' computed at five different model grid points, which are distributed from the center of convective activity to ~ 500 km southwest of Bermuda, following approximately the direction of the mean flow in layer 7. The positions of

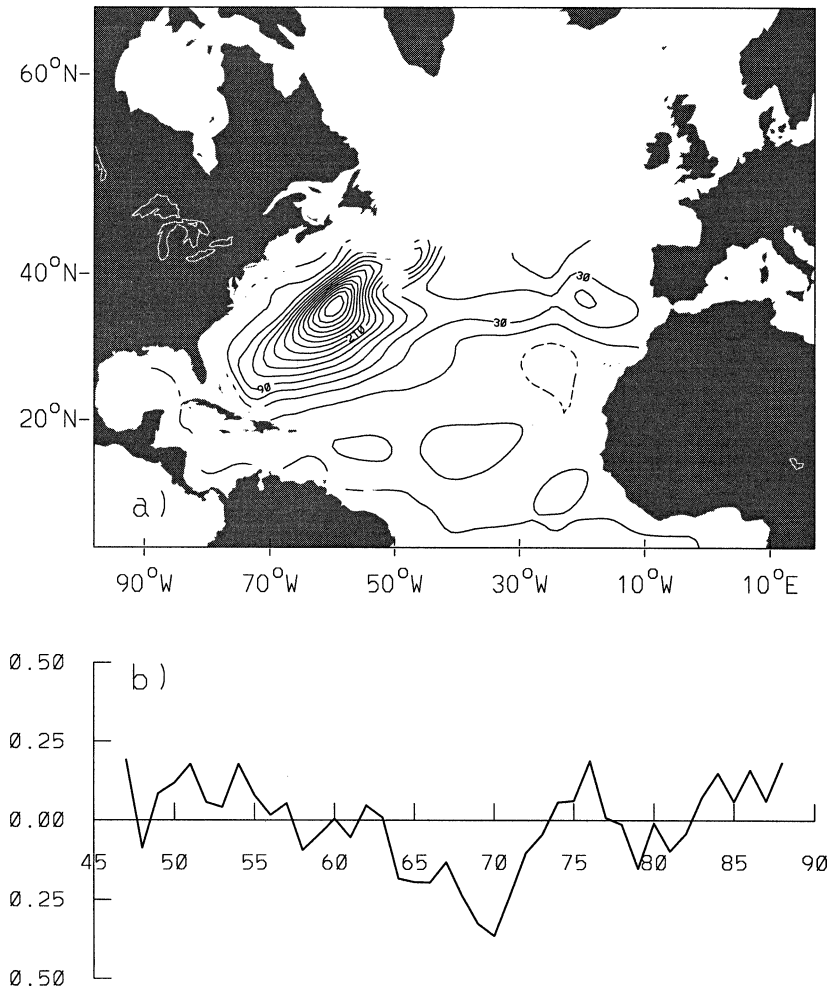


FIG. 7. (a) EOF 1 [solid (dashed) lines are positive (negative) contours; the contour interval is 30 m] and (b) time series of EOF 1 of the depth of the interface between layers 6 and 7 in Sep (EXPI).

these grid points are denoted by the circles along the line segment in Fig. 6b. The time lags between the different curves in Fig. 8 indicate a propagation speed on the order of 1 cm s^{-1} , which corresponds to the magnitude of the flow simulated in layers 6 and 7. The magnitude of the PV anomalies decays with time due to internal mixing (New et al. 1995).

Since the formation of STMW (and its low PV) is associated with intense wintertime buoyancy loss in the Gulf Stream region, the observed and simulated PV variability at Bermuda can be expected to be associated with variability in the surface buoyancy flux. However, previous investigators have found little correlation between the two quantities (Jenkins 1982; Talley and Raymer 1982). EXPII was designed to isolate the effects of surface heat flux anomalies by eliminating the mechanical response of the ocean to the wind stress anomalies. The time evolution of the PV' at Bermuda in EXPI and EXPII is compared in Fig. 9, which indicates that EXPII successfully simulates the near-decadal oscillation ob-

served in EXPI and in observations. The magnitude of PV' at Bermuda in EXPIII (which includes τ' but not the anomalies related to the thermodynamic forcing) is much smaller than in the other experiments, and can be recovered to a good approximation by subtracting the PV' in EXPII from that in EXPI.

In order to represent the variability of the surface heat flux in the western subtropical gyre, the average wintertime (January–March) heat flux anomaly (hereafter QF') was computed over a region extending from 28° to 40°N and 56° to 80°W, and is also shown in Fig. 9. There is little difference among the values of QF' computed from both of the model experiments and from observations, and the quantity shows only a small dependence upon the size of the area within which the average was computed. There is also good agreement between QF' and EOF1 HFLX (contrast Figs. 3b and 9). This indicates that both the averaged flux and the first EOF of the heat flux are representative of the surface heat flux variability in the western Atlantic. This

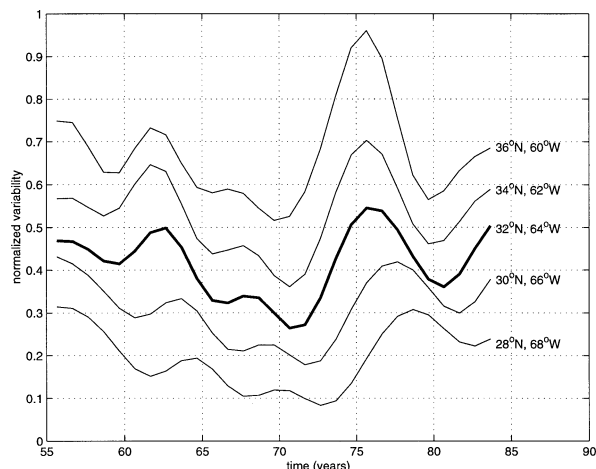


FIG. 8. STMW PV' (normalized by standard deviation) in the western subtropics, at the locations indicated in Fig. 6. A low-pass filter with a 5-yr cutoff frequency has been applied to PV' at each station, and the curves are offset by 0.15 standard deviation.

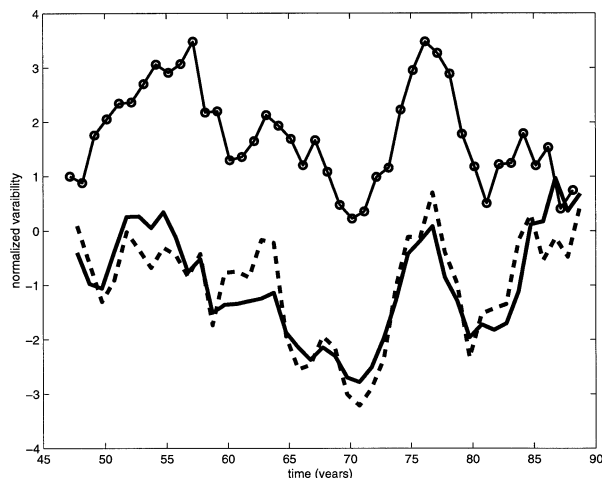


FIG. 10. STMW PV' at Bermuda in EXPI (dashed line) and EXPII (solid line) and the integrated wintertime downward surface heat flux anomaly in the western subtropics (solid line with circles). All curves are normalized by their respective standard deviations. The heat flux and the PV' curves are offset by two standard deviations.

also means that the area over which QF' is computed dominates the first EOF mode computed over the entire basin.

While there is some visual correlation between the anomalous atmospheric forcing (QF') and the variations of PV at Bermuda for near-decadal timescales (Fig. 9), the magnitude and phase of the simulated variability do not correlate well over the entire period. Talley and Raymer (1982), in a similar comparison using observations for the 1954–72 period, note that the apparent trend of weakening heat loss observed in the 1960s is not followed by an expected increase in PV' . In fact, a minimum in PV' was reached at the end of that decade. Those authors, however, presented their results in terms

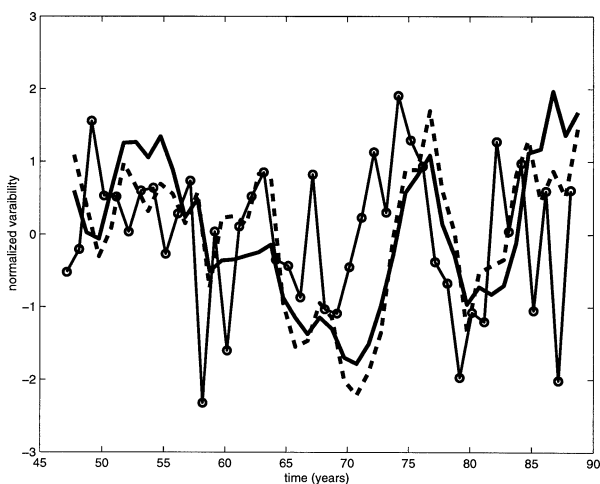


FIG. 9. STMW PV' at Bermuda in EXPI (dashed line) and EXPII (solid line) and the wintertime downward surface heat flux anomaly averaged within latitudes 28° – 40° N, longitudes 56° – 80° W (solid line with circles). All curves are normalized by their respective standard deviations.

of the total heat flux instead of its variability, and it is difficult to clearly distinguish from their figures all of the timescales associated with the heat flux and potential vorticity variability.

The results shown in Fig. 9, in which the heat flux and potential vorticity anomalies are compared, suggest that the PV' fields are not a direct response to the high (biannual) frequencies in the atmospheric forcing (QF'), as evident, for example, in the intense cooling events around 1960. It is therefore possible that long-term heat storage, associated with the tight recirculation in the Sargasso Sea, and preconditioning of the convective activity play an important role in the process of generating the observed and simulated STMW PV anomalies (Jenkins 1982). In order to verify this assumption, the integral effect of the heat flux anomalies over the western Atlantic has been computed by integrating QF' (from an arbitrary initial level) for the duration of the model experiments (Fig. 10). To a first approximation, the integrated heat flux anomalies, in which the importance of individual extreme events is minimized, correspond well with the PV anomalies at Bermuda. In particular, the high PV' in the early 1950s can be interpreted as an oceanic response to a succession of moderately warm winters, while the decreasing trend in PV' in the late 1950s and in the 1960s (as well as the magnitude of the PV' minimum in 1970) can be interpreted as a response to an integral cooling, resulting from a succession of anomalously cold winters. This analysis indicates that the STMW variability at near-decadal timescales can be explained, to a large extent, as an oceanic response to variations in the surface heat flux in the western subtropical Atlantic.

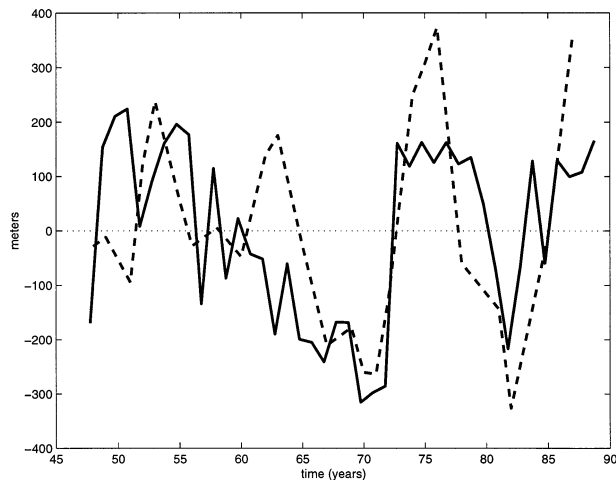


FIG. 11. Time evolution of model (EXPI) layer 12 thickness anomaly in the Labrador Sea (solid line) and of the thickness of the observed LSW core (dashed line, redrawn from Curry et al. 1998).

5. Variability in the Labrador Sea

The Labrador Sea is one of the major sites within which deep convection takes place in the North Atlantic. In the central Labrador Sea, this deep convection, driven primarily by intense wintertime heat loss to the atmosphere, leads to the production of the cold (and relatively fresh) LSW (Lazier 1981; Talley and McCartney 1982), with the thickness of the LSW core being directly proportional to the intensity of convection (Curry et al. 1998). In this section, the simulated variability in convective activity (and water mass formation) in the Labrador Sea is compared to observations, and its response to the surface forcing is investigated.

Under anomalous forcing, convection and water mass formation in the Labrador Sea undergo intense interannual and near-decadal variations in the model simulations. As discussed in Paiva and Chassignet (2001), ventilation in the model is very sensitive to the surface conditions. During the spinup phase, the simulation of slightly fresher and warmer surface wintertime conditions leads to the formation of a lighter than observed water mass in the Labrador Sea, with the mixed layer ventilating primarily layer 12 ($\sigma_\theta = 27.64$). The time evolution of the layer 12 thickness anomaly for EXPI (computed at the grid point closest to OWS Bravo) is shown in Fig. 11 and is compared to observations of LSW thickness. To a first approximation, the model is able to capture the phase and order of magnitude of the observed near-decadal variability, if not its maximum amplitude. In a manner similar to that in reality, the simulated water mass production in the Labrador Sea was reduced in the late 1960s and early 1980s, while intense convection in the early 1970s and around 1985, corresponding to the simulated negative SST anomalies, led to a restoration of the production levels observed in the 1950s. The mechanical effect of the wind stress anomalies (τ' in EXPIII) has only minor impact on the

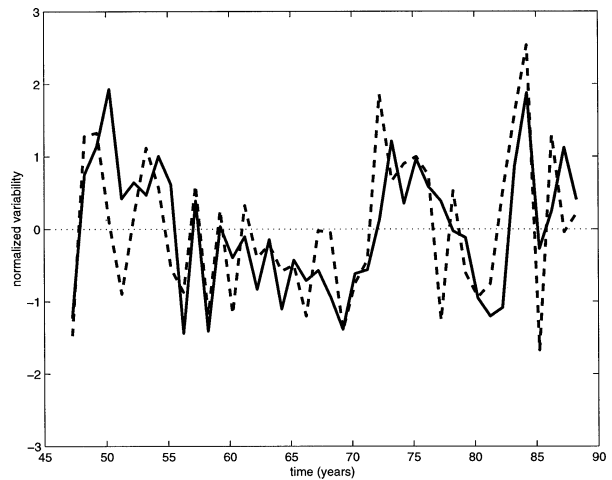


FIG. 12. Simulated March mixed layer depth anomaly at the position of OWS Bravo in the model in EXPI (solid line) and wintertime upward surface heat flux anomaly in the Labrador Sea (dashed line). Both curves are normalized by their respective standard deviations.

convective activity in the Labrador Sea, and EXPII, which does not include τ' , reaches results very similar to those of EXPI.

It is important to note that the observed advection of intense freshwater anomalies into the central Labrador Sea, corresponding to the great salinity anomaly of 1969–70 (Dickson et al. 1988) and the “lesser great salinity anomaly” of the early 1980s (Curry et al. 1998; Belkin et al. 1998), was not represented in the model. Accordingly, the simulated SSS variability is very small in comparison to that in the observations, and the simulated variability in convective activity is caused primarily by the surface heat flux variability. The anomalies of the simulated March mixed layer depth (representing the convective intensity) correlate reasonably well (correlation coefficient -0.67) with the wintertime (January–March average) heat flux anomalies averaged over the Labrador Sea (Fig. 12). This correlation is reduced for the heat flux computed for individual months (March anomalies, e.g., instead of seasonally averaged anomalies) but is not strongly dependent upon the size of the domain within which the fluxes are averaged.

6. Summary and discussion

In this study, the atmospherically forced low-frequency variability in water mass formation in the North Atlantic Ocean has been investigated in a realistic OGCM forced by COADS atmospheric fields from 1946 to 1988. In particular, this investigation addresses the questions of whether, and to what extent, realistic surface heat flux anomalies can generate the observed interannual and near-decadal variability in the convective activity of the western Atlantic basins and the observed potential vorticity anomalies of STMW and LSW.

The surface heat flux anomalies were indeed found

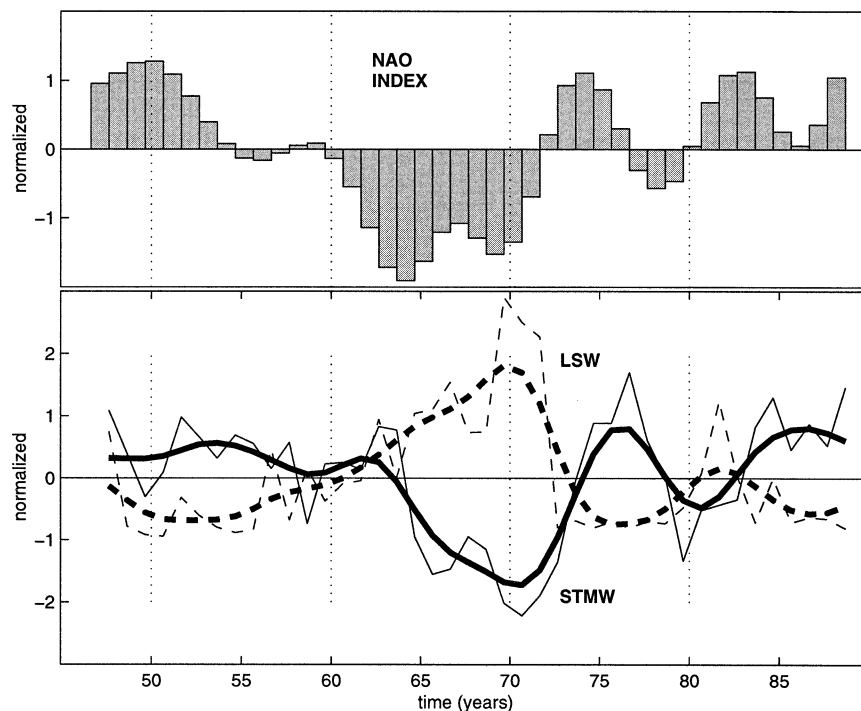


FIG. 13. Comparison between the NAO index of Hurrell (1999, personal communication), and the model (EXPI) LSW (dashed lines) and STMW (solid line) PV anomalies. Both PV' curves were low-pass filtered (thick lines) with the same weights (1, 3, 5, 6, 5, 3, 1) applied to the NAO index. All curves are normalized by their respective standard deviations.

to be the primary forcing mechanism that generated in the model near-decadal variations in the potential vorticity of the STMW and in the depth of isopycnal surfaces in the western subtropics, in good agreement with observations at the Panulirus station (Bermuda). The potential vorticity signals originated to the northeast of Bermuda and were advected by the mean flow through the location of the Panulirus station at speeds on the order of 1 cm s^{-1} , with their magnitude attenuated along the trajectory due to internal mixing. The horizontal scale of these western subtropics potential vorticity anomalies is on the order of $\sim 10^\circ$ lat by $\sim 15^\circ$ lon. The anomalies occupy most of the Sargasso Sea and are limited in the west-northwest direction by the Gulf Stream front. These results support those from observations (Molinari et al. 1997), which show that the temperature variability from the surface to 400 m is coherent over a large area of the western subtropics.

The simulated STMW potential vorticity signals are associated with changes in the buoyancy of the winter-time surface mixed layer, the timescales of which are represented in the first EOF modes of both the simulated heat flux and the SST anomalies in the model domain. Heat storage and preconditioning of the convective activity were shown to be the important factors for the generation of STMW variability with persistence of cold (warm) conditions, associated with anomalous heat loss (gain) over the western subtropics, being more signifi-

cant for the generation of the simulated variability than were strong anomalous events in isolated years. The residence time can be long in the recirculating waters of the western subtropical region east of the Gulf Stream, and the upper ocean has a “memory” of previous years.

In the Labrador Sea, the model was able to capture the phase and order of magnitude of the observed near-decadal variability in the convective activity, if not its maximum amplitude. The agreement between model and observations, despite the absence in the simulations of the freshwater anomalies of 1969–70 and early 1980s, highlights the importance of the surface heat flux variability in driving the observed convective anomalies. Dickson et al. (1996) have pointed out that the generation and advection of the Great Salinity Anomaly and the surface heat fluxes in the Labrador Sea are connected phenomena, associated with the NAO.

At near-decadal timescales, the PV anomalies of STMW at Bermuda and of LSW near OWS Bravo are consistently out of phase with one another in the model simulations (Fig. 13) as well as in the observations. When time series of PV' are calculated for a region located to the northeast of Bermuda (where STMW is actually formed in the model), this out-of-phase character can also be extended, to a certain degree, to interannual timescales (not shown). This asynchronicity in the water mass formation in the western subtropics

and in the Labrador Sea is consistent with the dipole pattern of the wintertime SST (and buoyancy) anomalies in the North Atlantic. In order to characterize the time-scales associated with the atmospheric variability (and with the anomalous forcing in the model), the NAO index from Hurrell (1999, personal communication) is also shown in Fig. 13. While the NAO presents near-decadal oscillations very similar to the PV' (for both STMW and LSW), there is an indication that PV' lags the NAO index by approximately 2–3 years, indicative of the slow oceanic response time to the atmospheric forcing (Curry et al. 1998).

Variability of the NAO represents changes in the pattern of the large-scale atmospheric circulation, which generate anomalous sensible and latent heat flux by modifying the strength and position of the westerly winds and the advection of heat and moisture over the ocean. When the NAO is high, strong winds and continental cold air advection (associated with the north-westerly component of the winds) over the Labrador Sea intensify the heat loss to the atmosphere (Dickson et al. 1996), coinciding with periods of intense convection and low LSW PV' (Fig. 13). At the same time, inflow of warm and moist oceanic air reduces latent heat loss (the dominant component of the surface heat flux from the tropics to midlatitudes) in the western subtropics (Cayan 1992; Zorita et al. 1992), which is followed by low production (and high PV') of STMW. When the NAO is low, the Atlantic storm track shifts southward along with the westerlies (Rogers 1990; Joyce et al. 2000), intensifying the outbreaks of cold and dry continental air over the western subtropics (Marsh and New 1996) and increasing the latent heat loss in that region, and the strongest renewal (and lowest PV') of STMW are simulated (and observed) at Bermuda (Fig. 13). Reduction of convection in the Labrador Sea (and high LSW PV') accompanies the reduced heat loss during the low NAO periods.

These results support the idea that the variability in water mass formation in the western North Atlantic can be attributed, to a large extent, to changes in the pattern of the large-scale atmospheric circulation, which generate sensible and latent heat flux variability by modifying the strength and position of the westerly winds and the advection of heat and moisture over the ocean. To our knowledge, this is the first time that the interannual and near-decadal subsurface variability associated with STMW and LSW, and its relationship to the NAO, has been simulated in an ocean general circulation model.

The present work represents an attempt to simulate and to understand the oceanic subsurface low-frequency variability within the framework of an ocean-only model. This approach precludes an investigation of possible coupling mechanisms, by which the simulated oceanic state could feed back upon the atmospheric circulation. By restricting the coupling with the atmosphere, however, it becomes possible to investigate the ocean re-

sponse to specific forcing mechanisms, such as in this study the impact of surface heat flux anomalies upon the water mass formation. It is the ability to retain a large degree of realism while isolating important physical mechanisms in process-oriented studies, combined with a spatial and temporal coverage that is ordinarily absent from observations, that makes OGCMs an essential tool for the investigation of the ocean climate and its variability.

Acknowledgments. The authors wish to thank L. Smith for her careful editing of the manuscript. This research was supported by the National Science Foundation through Grants OCE-9531852 and OCE-0000042. The first author was also supported by a fellowship from Conselho Nacional de Desenvolvimento Científico e Tecnológico (CNPq).

REFERENCES

- ACCP, 1992: The Atlantic Climate Change Program. Proceedings from the principal investigators meeting. J. J. Cione, Ed., NOAA Climate and Global Change Program, Special Rep. 7, 168 pp.
- Alexander, M. A., and C. Deser, 1995: A mechanism for the recurrence of wintertime midlatitude SST anomalies. *J. Phys. Oceanogr.*, **25**, 122–137.
- , and —, 1997: Surface flux variability over the North Pacific and North Atlantic Oceans. *J. Climate*, **10**, 2963–2978.
- Battisti, D. S., U. S. Bhatt, and M. A. Alexander, 1995: A modeling study of the interannual variability in the wintertime North Atlantic Ocean. *J. Climate*, **8**, 3067–3083.
- Belkin, I. M., S. Levitus, J. Antonov, and S.-A. Malmberg, 1998: Great salinity anomalies in the North Atlantic. *Progress in Oceanography*, Vol. 41, Pergamon, 1–68.
- Bjerknes, J., 1964: Atlantic air–sea interaction. *Advances in Geophysics*, Vol. 10, Academic Press, 1–82.
- Bleck, R., and E. Chassignet, 1994: Simulating the oceanic circulation with isopycnic-coordinate models. *The Oceans: Physical-Chemical Dynamics and Human Impact*, S. K. Majumdar, E. W. Miller, G. S. Forbes, R. E. Schmalz, and A. A. Panah, Eds., The Pennsylvania Academy of Science, 17–39.
- , C. Rooth, D. Hu, and L. T. Smith, 1992: Salinity-driven thermocline transients in a wind- and thermohaline-forced isopycnic coordinate model of the North Atlantic. *J. Phys. Oceanogr.*, **22**, 1486–1505.
- Cayan, D. R., 1992: Latent and sensible heat flux anomalies over the northern oceans: Driving the sea surface temperature. *J. Phys. Oceanogr.*, **22**, 859–881.
- Curry, R. G., M. S. McCartney, and T. M. Joyce, 1998: Oceanic transport of subpolar climate signals to mid-depth subtropical waters. *Nature*, **391**, 575–577.
- da Silva, A. M., C. C. Young, and S. Levitus, 1994: *Algorithms and Procedures*. Vol. 4, *Atlas of Surface Marine Data*, NOAA Atlas NESDIS 8, 83 pp.
- Delworth, T. L., 1996: North Atlantic interannual variability in a coupled ocean–atmosphere model. *J. Climate*, **9**, 2356–2375.
- Deser, C., and M. L. Blackmon, 1993: Surface climate variations over the North Atlantic Ocean during winter: 1900–1989. *J. Climate*, **6**, 1743–1753.
- Dickson, R. R., and J. Namias, 1976: North American influences on the circulation and climate of the North Atlantic sector. *Mon. Wea. Rev.*, **104**, 1255–1265.
- , J. Meincke, S. A. Malmberg, and A. J. Lee, 1988: The “Great Salinity Anomaly” in the northern North Atlantic 1968–1982. *Progress in Oceanography*, Vol. 20, Pergamon, 103–151.
- , J. Lazier, J. Meincke, P. Rhines, and J. Swift, 1996: Long-term

- coordinated changes in the convective activity of the North Atlantic. *Progress in Oceanography*, Vol. 38, Pergamon, 241–295.
- Fioux, M., and H. Stommel, 1975: Preliminary look at feasibility of using marine reports of sea surface temperature for documenting climatic change in the western North Atlantic. *J. Mar. Res.*, **33**, 83–95.
- Häkkinen, S., 1999: Variability of the simulated meridional heat transport in the North Atlantic for the period 1951–1993. *J. Geophys. Res.*, **104**, 10 991–11 007.
- Halliwel, G. R. J., 1998: Simulation of North Atlantic decadal/multi-decadal winter SST anomalies driven by basin-scale atmospheric circulation anomalies. *J. Phys. Oceanogr.*, **28**, 5–21.
- Hazeleger, W., and S. S. Drijfhout, 1998: Mode water variability in a model of the subtropical gyre: Response to anomalous forcing. *J. Phys. Oceanogr.*, **28**, 266–288.
- Houghton, R. W., 1996: Subsurface quasi-decadal fluctuations in the North Atlantic. *J. Climate*, **9**, 1363–1373.
- Jenkins, W. J., 1982: On the climate of a subtropical ocean gyre: Decade time scale variations in water mass renewal in the Sargasso Sea. *J. Mar. Res.*, **42**, 265–290.
- Joyce, T. M., and P. Robbins, 1996: The long-term hydrographic record at Bermuda. *J. Climate*, **9**, 3121–3131.
- , C. Deser, and M. A. Spall, 2000: The relation between decadal variability of subtropical mode water in the North Atlantic and large-scale patterns of air–sea forcing. *J. Climate*, **13**, 2550–2569.
- Kushnir, Y., 1994: Interdecadal variations in North Atlantic sea surface temperature and associated atmospheric conditions. *J. Climate*, **7**, 141–157.
- Latif, M., and T. P. Barnett, 1994: Causes of decadal climate variability over the North Pacific and North America. *Science*, **266**, 634–637.
- Lazier, J. R. N., 1981: Oceanographic conditions at O.W.S. Bravo. *Atmos.–Ocean*, **18**, 227–238.
- , 1988: Temperature and salinity changes in the deep Labrador Sea, 1962–1986. *Deep-Sea Res.*, **35**, 1247–1253.
- Levitus, S., 1982: *Climatological Atlas of the World Ocean*. NOAA Prof. Paper No. 13, 173 pp. and 17 microfiche.
- , 1989: Interpentadal variability of temperature and salinity at intermediate depths of the North Atlantic Ocean, 1970–1974 versus 1955–1959. *J. Geophys. Res.*, **94**, 6091–6131.
- Luksch, U., and H. von Storch, 1992: Modeling the low-frequency sea surface temperature variability in the North Pacific. *J. Climate*, **5**, 893–906.
- Marsh, R., and A. L. New, 1996: Modeling 18°C water variability. *J. Phys. Oceanogr.*, **26**, 1059–1080.
- Marshall, J., and F. Schott, 1999: Open-ocean convection: Observations, theory and models. *Rev. Geophys.*, **37**, 1–64.
- Marshall, J. C., A. J. G. Nurser, and R. G. Williams, 1993: Inferring the subduction rates and period over the North Atlantic. *J. Phys. Oceanogr.*, **23**, 1315–1329.
- McCartney, M. S., 1982: The subtropical recirculation of mode waters. *J. Mar. Res.*, **40** (Suppl.), 427–464.
- , and L. D. Talley, 1982: The bipolar mode water of the North Atlantic Ocean. *J. Phys. Oceanogr.*, **12**, 1169–1188.
- Miller, A. J., D. R. Cayan, and W. B. White, 1998: A western-intensified decadal change in the North Pacific thermocline and gyre-scale circulation. *J. Climate*, **11**, 3112–3127.
- Molinari, R. L., D. A. Mayer, J. F. Festa, and H. F. Bezdek, 1997: Multi-year variability in the nearsurface temperature structure of the mid-latitude western North Atlantic Ocean. *J. Geophys. Res.*, **102**, 3267–3278.
- New, A. L., R. Bleck, R. Marsh, M. Huddleston, and S. Barnard, 1995: An isopycnic model study of the North Atlantic. Part 1: Model experiment. *J. Phys. Oceanogr.*, **25**, 2667–2699.
- Paiva, A. M., and E. P. Chassignet, 2001: Impact of surface flux parameterization on the modeling on the North Atlantic Ocean. *J. Phys. Oceanogr.*, **31**, 1860–1879.
- Perry, G. D., P. B. Duffy, and N. L. Miller, 1996: An extended data set of river discharges for validation of general circulation models. *J. Geophys. Res.*, **101**, 21 339–21 349.
- Rogers, J. C., 1990: Patterns of low-frequency monthly sea-level pressure variability (1899–1986) and associated wave cyclonic frequencies. *J. Climate*, **3**, 1364–1379.
- Sato, O. T., and T. Rosby, 1995: Seasonal and low frequency variations in the dynamic height anomaly and transport of the Gulf Stream. *Deep-Sea Res.*, **42**, 149–164.
- Seager, R., Y. Kushnir, and M. A. Cane, 1995: On heat flux boundary conditions for ocean models. *J. Phys. Oceanogr.*, **25**, 3219–3230.
- , —, M. Visbeck, N. Naik, J. Miller, G. Krahnemann, and H. Cullen, 2000: Causes of Atlantic Ocean climate variability between 1958 and 1998. *J. Climate*, **13**, 2845–2862.
- Talley, L. D., 1996: North Atlantic circulation and variability reviewed for the CNLS conference. *Physica D*, **98**, 625–646.
- , and M. S. McCartney, 1982: Distribution and circulation of Labrador Sea Water. *J. Phys. Oceanogr.*, **12**, 1189–1205.
- , and M. E. Raymer, 1982: Eighteen degree water variability. *J. Mar. Res.*, **40** (Suppl.), 757–775.
- WCRP, 1995: CLIVAR: A study of climate variability and predictability. World Climate Research Programme Tech. Rep. WCRP-89, WMO/TD 690, 157 pp.
- Worthington, L. V., 1959: The 18 Degree Water in the Sargasso Sea. *Deep-Sea Res.*, **5**, 297–305.
- , 1977: Intensification of the Gulf Stream after the winter of 1976–77. *Nature*, **270**, 415–417.
- Zhang, R.-H., L. M. Rothstein, and A. J. Busalacchi, 1998: Origin of upper-ocean warming and El Niño change on decadal scales in the tropical Pacific Ocean. *Nature*, **391**, 879–883.
- Zorita, E., V. Kharin, and H. van Storch, 1992: The atmospheric circulation and sea surface temperature in the North Atlantic area in winter: Their interaction and relevance for Iberian precipitation. *J. Climate*, **5**, 1097–1108.